Epitaxial growth of fcc Ti films on Al(001) surfaces

Adli A. Saleh,* V. Shutthanandan,† N. R. Shivaparan, and R. J. Smith
Department of Physics, Montana State University, Bozeman, Montana 59717

T. T. Tran and S. A. Chambers
Environmental Molecular Sciences Laboratory, Pacific Northwest National Laboratory, Richland, Washington 99352
(Received 27 May 1997)

High-energy ion scattering (HEIS), x-ray photoelectron spectroscopy, and x-ray photoelectron diffraction (XPD) were used to study the growth of thin Ti films on Al(001) surfaces. The Al surface peak area in the backscattered ion spectrum of MeV He^+ ions, incident along the [001] direction, was used to monitor the atomic structure of the Ti films during growth. An initial decrease in the area was observed indicating epitaxial film growth. This decrease continued up to a critical film thickness of about 5.5 ML, after which point the structure of the film changed. Titanium films 3, 5, and 9 ML thick were characterized using XPD in the *same* chamber. Both the HEIS and XPD results show that the Ti films grow with an fcc structure on Al(001). A tetragonal distortion of 2.4% in the fcc Ti film was measured using ions incident along the [101] direction. Although there is a general similarity of fcc Ti growth on both Al(001) and Al(110), the submonolayer growth regime does show differences for the two surfaces. [S0163-1829(97)03940-4]

INTRODUCTION

In an earlier paper we presented a study of the epitaxial growth of metastable fcc Ti films on Al(110) surfaces at room temperature.[1] Similar studies on the growth of other transition metals, Pd, Ni, and Fe, show that the nature of the growth may be dependent on the Al substrate surface orientation. On one hand, Pd films intermix with both Al(001) and Al(110) surfaces to form an AlPd-like phase at the Al-Pd interface.[2,3] On the other hand, thin Ni films intermix with the Al(110) surface to form an AlNi-like phase, but tend to form a Ni overlayer on the Al(001) surface.[4,5] A recent study of thin Fe films deposited on Al surfaces indicated the growth of an AlFe-like phase at the interface, although Fe growth on Al(110) appeared to have a more Al-rich initial phase at the interface.[6] In this paper we show that Ti grows epitaxially on the Al(001) surface, similar to the behavior observed on the Al(110) surface. There are, however, some differences for the first monolayer of Ti deposition. In addition, we use off-normal ion channeling to measure the distortion of the fcc Ti lattice associated with the epitaxial lattice matching, and compare our results with a recent quantitative low-energy electron diffraction (LEED) analysis of this system.[7] We also present photoelectron diffraction measurements to further confirm the existence of an fcc structure in the Ti overlayer. Understanding the growth of these epitaxial Ti films will benefit our knowledge of metal-metal epitaxy, and is expected to have applications in the development of diffusion barriers and metallization schemes on electronic materials.

EXPERIMENTAL TECHNIQUES

High-energy ion scattering (HEIS) and x-ray photoelectron spectroscopy (XPS) were the primary techniques used in this study. When used in the channeling mode, HEIS provides a powerful tool to probe the substrate surface structure as well as the overlayer structures and growth modes.[8,9] Ion scattering also provides a direct means for accurately measuring the overlayer coverage when the ion beam is incident on the substrate in a random direction. In the channeling geometry the ion beam is incident along a low-index crystallographic direction, and the energy spectrum of backscattered particles exhibits a surface peak (SP) associated with ions backscattered from the topmost layers of the solid. The SP areas are converted to areal densities of visible target atoms (atoms/cm^2) using the Rutherford-scattering cross section, the solid angle subtended by the detector, and the time-integrated incident ion current. To extract information about the surface structure from the data, the experimentally measured ion yields are compared with the scattering yields calculated using computer simulations of the channeling measurements for various overlayer-substrate structures. In the XPS experiments the attenuation of the Al photopeak intensity as a function of Ti coverage is used to characterize the morphology of the Ti films. Photoemission is also used to determine the amount of contamination on the sample surface during the cleaning process. To better characterize the structure of the epitaxial film, off-normal channeling measurements were performed to determine the Ti(001) interplanar distance in the overlayer. Scanned-angle photoelectron diffraction measurements (XPD) confirmed the fcc structure of the Ti overlayer determined by ion scattering. To our knowledge, this study was the first attempt to compare the results from both XPD and HEIS techniques in the same vacuum system with the same sample.

The Al single crystals were cut and polished to within 0.5° of the (001) crystallographic plane, as measured using x-ray diffraction. The crystals were then chemically etched for 15 sec in an aqueous solution containing HCl(1.5%), HF(1.5%), and HNO_3(2.5%), and mounted in the UHV chamber. Three strands of high-purity Ti wires (99.99%), 0.25 mm in diameter and 10 cm in length, were twisted together, wound into small coils, and then etched in a 20%

HF solution. To deposit Ti on the Al surfaces in vacuum these filaments were resistively heated using a constant current supply to maintain a constant Ti sublimation rate. The Ti filaments were mounted 5 in. away from the Al sample so that a uniform Ti flux was obtained across the sample surface. A deposition rate of about 0.5 ML/min, as measured by ion scattering, was obtained by maintaining a current of 4.5 A through the Ti wire. On the Al(001) surface one monolayer (ML) is 1.22×10^{15} atoms/cm^2. All Ti depositions were performed with the Al sample at room temperature.

The UHV chamber used for the HEIS measurements is connected to a 2-MV Van de Graaff accelerator through a differentially-pumped beam line as described elsewhere.[10] The Al crystal was mounted in the chamber on a thick Mo block which is attached to a three-axis goniometer for channeling measurements. The temperature of the Mo block was monitored using a calibrated Pt resistor mounted inside of the block. After baking the UHV system, a pressure of 1.5×10^{-10} Torr was obtained. Energy analysis of the backscattered particles for HEIS was performed using a bakeable, passivated, implanted planar silicon detector installed on a rotatable arm and located 3 in. away from the sample. The detector position was set at a scattering angle of 105° for these experiments.

In vacuum the crystals were cleaned by repeated cycles of 1–1.5 keV Ar^+ ion bombardment for several hours with the sample at room temperature, followed by annealing the sample at 450 °C for 15 min. The cleaning procedure was repeated until the photopeak associated with aluminum oxide was completely removed from the XPS spectrum. The O 1*s* photopeak could not be used to reliably monitor the Al surface oxide because the XPS analysis area included a small portion of the Mo sample holder surrounding the Al crystal. After cleaning the sample, a collimated beam of He^+ ions, passing through an aperture of 1.2 mm^2 area, was used to carry out the ion scattering measurements. The sample was aligned with the ion beam incident along the [001] direction by minimizing the backscattered ion yield in a small region behind the surface peak.

Ion scattering and XPS measurements were made after each Ti deposition. A total dose of 1.56×10^{15} ions/cm^2 was used to collect each HEIS spectrum. In a preliminary experiment to measure the damage induced by the incident He^+ beam, no significant increase in ion yield was observed after an ion dose of 3.1×10^{16} ions/cm^2. In addition, an ion scattering spectrum was measured, however, less frequently, with the sample rotated out of the channeling alignment to determine the total Ti coverage at the different stages of the experiment. These measurements in a random-alignment geometry eliminate possible errors, associated with the shadowing of Ti atoms, in determining the Ti coverage. The uncertainty in the ion scattering yields reported here is estimated to be $\pm5.6\%$ with the largest contribution to the uncertainty coming from the determination of the detector solid angle, and smaller contributions coming from uncertainties in the integrated charge, the scattering angle, and the determination of the surface peak area.

Ti and Al 2*p* core-level photopeaks were also monitored during the film growth using an Al $K\alpha$ x-ray source. A fixed pass energy of 50 eV and a scanning rate of 0.1 eV/s were used for the hemispherical analyzer (VSW HA 100). The angle between the sample normal and the electrostatic analyzer was fixed at $\theta=30°$ for the intensity versus coverage measurements. The acceptance angle of the analyzer is specified by the manufacturer to be $\pm6°$. Film deposition, channeling measurements, and XPS photopeak intensity measurements were all performed without moving the sample, although the sample was occasionally rotated slightly to measure the random alignment backscattering yield from Ti atoms. This arrangement helped in maintaining the sample alignment with the ion beam. In addition, for a 5-ML film, channeling measurements near the [101] direction (rocking curve) were done to determine the (001) interplanar distance in the Ti overlayer.

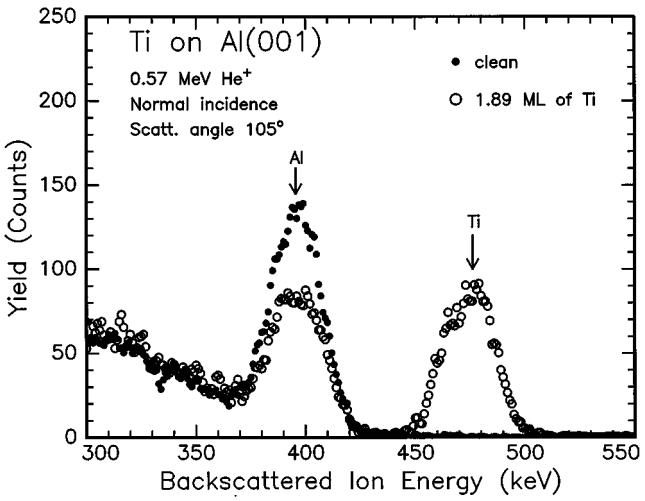

FIG. 1. He^+ ion backscattering spectra at 0.57 MeV incident ion energy along the [001] direction for a clean Al(001) surface (solid circles) and after a deposition of 1.89 ML of Ti. The Al and Ti surface peak energies are indicated by the vertical arrows.

After the initial experiments to characterize the Ti films as a function of Ti coverage, XPD measurements were made for Ti films with thicknesses of 3, 5, and 9 ML. The angular dependence of the photopeak intensities associated with Ti and Al core levels was used to complement the channeling measurements. The dependence of the intensities on the polar emission angle θ in the (010) azimuthal plane, over an angular range of 0°–55° off normal was measured for the clean Al substrate and for each of the three Ti films. Azimuthal angle scans of the photopeak intensities at $\theta=45°$ were also recorded. The scanning was accomplished by rotating the sample in a fixed-analyzer-source geometry with angular increments of 1°. For each point in the angular scan, the binding energy ranges that include the peaks of interest were scanned. Finally, single-scattering, spherical-wave calculations of the XPD scans, using the Rehr-Albers formalism,[11] were made and compared with the measurements to extract structural information about the Ti films which could be compared with the HEIS results.

RESULTS

A. HEIS measurements

Channeling spectra taken for the clean Al surface, and after the deposition of 1.89 ML of Ti, are shown in Fig. 1.

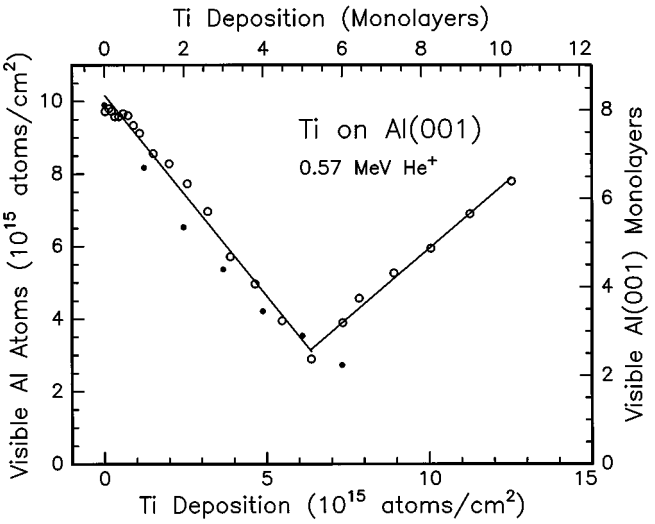

FIG. 2. Visible Al atoms, at 0.57 MeV incident ion energy, as a function of Ti coverage deposited at room temperature on the Al(001) surface (open circles). The solid circles indicate the yield for a flat pseudomorphic fcc Ti film, calculated using the VEGAS simulation code. The solid lines are linear fits to the two regions indicated, and are provided to guide the eye.

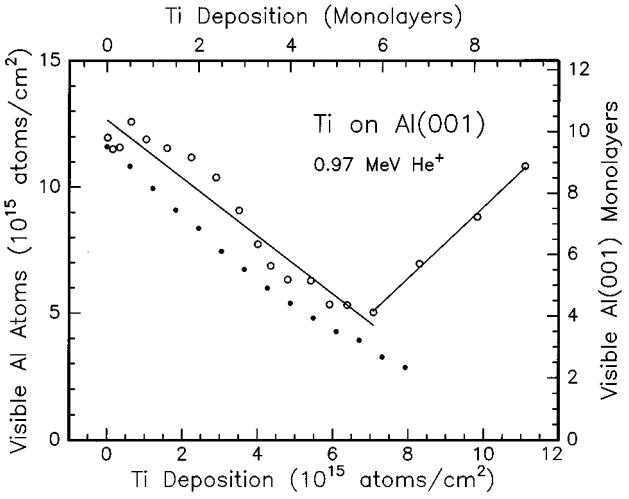

FIG. 3. Visible Al atoms, at 0.97 MeV incident ion energy, as a function of Ti coverage deposited at room temperature on the Al(001) surface. The solid circles indicate the yield for a flat, pseudomorphic Ti film, calculated using the VEGAS simulation code. The solid lines are linear fits to the two regions indicated, and are provided to guide the eye.

Both spectra were taken with the 0.57 MeV He^+ ion beam incident along the [001] direction, i.e., at normal incidence. The crystal was aligned by minimizing the integrated backscattering yield to the left of the SP in Fig. 1. The measured SP area yields a value of 9.7×10^{15} atoms/cm^2 for the clean (001) surface, or 4.0 Al atoms/row visible to the incident ion beam normal to the surface. This value is in excellent agreement with computer simulations for the clean surface, as discussed below. After deposition of 1.89 ML of Ti, the Al yield has *decreased* to 8.3×10^{15} atoms/cm^2, associated with the shadowing of Al surface atoms by Ti adatoms.

Figure 2 illustrates the basic growth characteristics of the Ti films on the Al(001) surface as measured using ion channeling. The open circles in the figure represent the experimental yield from Al atoms, i.e., the Al SP area from Fig. 1, plotted as a function of the Ti coverage as determined from the Ti yield in the ion scattering spectra recorded for a *nonchanneling* direction of incidence. For the first half monolayer of Ti coverage the trend in the SP area is not very clear, and may be assumed to be constant to within the experimental uncertainty. However, after this coverage and up to 5.5 ML of Ti deposited on the substrate, a decrease in the Al SP area was observed. An increase in the Al peak area is observed at higher Ti coverages. This behavior contrasts remarkably with the behavior for Pd, Ni, and Fe on Al(001) where the Al SP area *increases immediately* with metal deposition.[2–6]

Results of computer simulations of the ion scattering experiment are indicated by the solid circles in Fig. 2. The simulations were done using the VEGAS code with lattice parameters for bulk Al.[12,13] In these simulations the Ti atoms were arranged in a flat overlayer and placed on the Al fcc lattice sites above the Al surface. The Al(001) interplanar distance of 2.025 Å, and the Al vibration amplitude of 0.105 Å were used in simulating the Ti overlayer.[13]

We also carried out channeling measurements at higher incident ion energies to compare the SP changes with our previous results for Ti on Al(110),[1] and other metals on Al surfaces.[2–6] In Fig. 3 we show the backscattered ion yield for 0.97 MeV He^+ ions incident normal to the Al(001) surface. Shadowing of Al atoms is seen again for Ti coverages up to 5.5 ML, although the onset of shadowing at low coverages is less pronounced. At this higher ion energy our value for the clean Al SP yield is 11.95×10^{15} atoms/cm^2, or 4.9 Al atoms per row, somewhat larger than the value of 4.6 Al atoms/row reported previously.[14] Computer simulations (VEGAS) for layer-by-layer Ti growth are shown by the solid circles in Fig. 3, using the same lattice parameters as used in the calculations for Fig. 2.

After the experiments leading to the results of Fig. 3 were completed, the Al surface was cleaned and new Ti films were deposited with thicknesses of 3 and 5 ML, respectively. With these films the Ti and Al rocking curves were measured with the ion beam incident near the [101] direction, i.e., 45° from normal incidence. In the 3-ML experiment the measured variation in Ti SP area is quite small because of the lack of appreciable shadowing for our incident ion energy. For the 5 ML Ti film the Ti and Al rocking curves are shown in Fig. 4. The Ti yield (open circles) represents the variation in the SP area as a function of the angle between the sample normal and the incident ion beam. The Al bulk dechanneling yields, measured behind the SP and indicated by the closed circles in Fig. 4, were used to plot the Al rocking curve. The Al and Ti yields were normalized by dividing each measurement by the maximum backscattered yield measured in the experiment. The solid lines through the points are provided to guide the eye. As we shall see, these measurements were used to determine the interplanar distance of the epitaxial Ti overlayers.

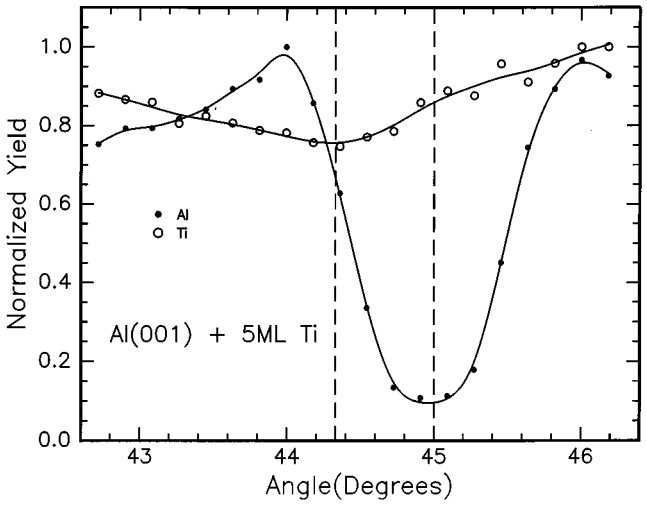

FIG. 4. The normalized Ti surface peak area (open circles) and the Al bulk dechanneling yield (solid circles) as a function of the angle of incidence near the [101] direction.

B. X-ray photoemission and photoelectron diffraction measurements

Figure 5 shows the Al $2p$ photopeak area, normalized to the value for the clean surface, plotted as a function of Ti coverage as determined from the ion scattering yield. The attenuation in the Al photopeak is not significant until the Ti coverage exceeds a thickness of about 1 ML. After this coverage the photopeak decreased in area throughout the experiment. The decay in the Al peak area is compared with an exponential decay represented by the solid curve as discussed in the next section. The data deviate slightly from this decay at higher Ti coverages.

The dependence of the Ti and Al photopeak areas was measured as a function of polar and azimuthal emission angles for the clean Al surface and for Ti films of 3, 5, and 9

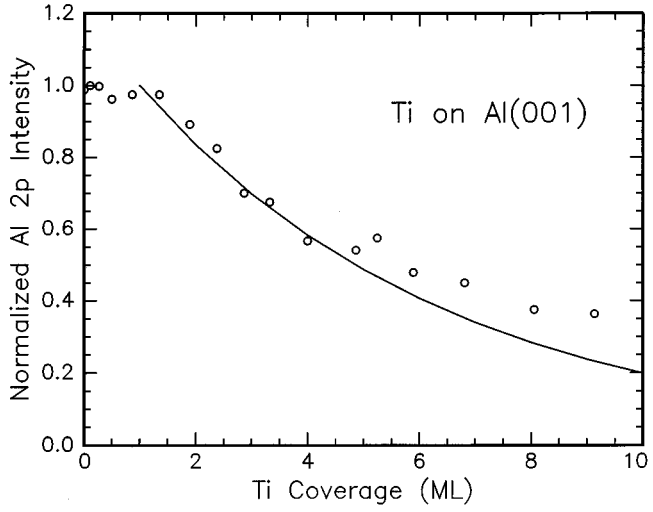

FIG. 5. Normalized Al $2p$ photoelectron intensities plotted as a function of Ti coverage on the Al(001) surface. The solid line is a model calculation for a layer-by-layer growth mode, using an attenuation length of 13 Å, for the data between 1 and 5.5 ML as discussed in the text.

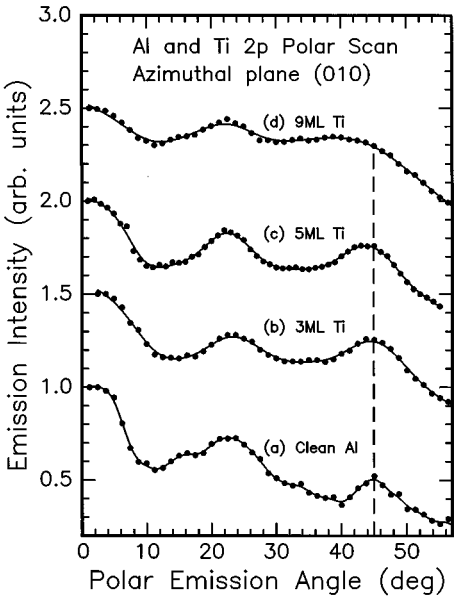

FIG. 6. Normalized Al and Ti $2p$ photoelectron intensities plotted as a function of polar emission angle along the [010] azimuth in the surface for (a) clean Al, and (b–d) three Ti coverages on the Al(001) surface, as indicated in the figure. The solid curves are provided to guide the eye.

ML thickness. The bottom curve in Fig. 6 shows the Al $2p$ photopeak polar scan in the (010) polar plane. The emission intensity, after background subtraction, has been normalized by the maximum value at zero polar angle. The curves in Fig. 6 have also been shifted vertically for clarity. The photopeak intensity for the clean Al surface is enhanced along several low-index directions of the crystal. The enhancements at $\theta=0°$ and 45° are associated with the central diffraction peaks in the [001] and [101] directions, respectively.[15] These two peaks are often referred to as ''forward focusing'' peaks. The structure at an angle of about 25° is due to a combination of first-order diffraction associated with forward scattering along [001] and [101], and forward focusing in the [103] direction.

The angular distributions of the photopeaks were measured again after the deposition of the Ti films. Curve (b) in Fig. 6 shows the Ti $2p$ photopeak polar scan for the 3 ML Ti film as compared to that of the clean Al $2p$ photopeak. The Ti photopeak distribution clearly exhibits enhanced emission in the [001] and [101] directions coinciding with peaks for the Al $2p$ level in curve (a). The polar emission distribution curve obtained for the 5 ML Ti film is shown as curve (c) in Fig. 6. The angular position of the enhancement near [101] is slightly shifted to the left of the vertical dashed line, placed at 45°. These results generally agree with the observation that the angular location of the minima in the Ti and Al rocking curves (Fig. 4) do not coincide.

The ion scattering results presented earlier suggest that there is a change in film structure for Ti coverages exceeding 5.5 ML. The photoelectron diffraction measurements support this picture at least for a 9 ML Ti film, as shown as curve (d) in Fig. 6. Although some forward focusing along [001] is still present, the emission along [101] is much less distinct than that measured for the thinner Ti films. In Fig. 5 we see

that the Al $2p$ photoemission intensity continues to decrease for Ti coverages greater than 5.5 ML so there is no evidence for Ti island formation or Al diffusion into the overlayer, both of which would lead to an increase of Al XPS intensity.

DISCUSSION OF RESULTS

There are two major growth regimes for Ti films on the Al(001) and Al(110) surfaces as seen in Fig. 2 and Ref. 1. The emphasis in this work is to characterize the growth below 5.5 ML, and to compare the growth for the two Al surfaces. We do this by considering first the HEIS results and subsequently the XPS and XPD results. We also note the differences for the two surfaces in the submonolayer coverage regime, and return to this point at the end of the discussion.

In the coverage regime between 1 and 5.5 ML an epitaxial, nearly fcc structure is observed for the Ti films. The primary evidence for this is the reduction in Al yield, seen in Fig. 2, which can only occur if Ti atoms sit directly above Al atoms in a pseudomorphic structure. Any other arrangement of Ti atoms will not result in this amount of Al shadowing. Similar behavior was seen for Ti films on Al(110).[1] However, for the (110) surface the shadowing was apparent even at submonolayer Ti coverages, while on the (001) surface there is an apparent coverage delay before Al shadowing occurs. The delay is also manifested in the lack of attenuation in the Al $2p$ photopeak at low Ti coverages shown in Fig. 5. This behavior is consistent with the formation of a Ti-Al alloy in the surface layer on Al(001).

After the critical thickness of 5.5 ML is reached, we believe that the strain energy in the Ti film exceeds the Ti-Al interfacial energy, resulting in the interruption of pseudomorphic growth. Although the atomic structure after 5.5 ML cannot be completely determined on the basis of our results, we believe that misfit dislocations in the thicker Ti films allow Ti atoms to gradually shift parallel to the surface, relieving strain in the film, uncovering Al atoms in the substrate, and causing the Al yield to slowly increase back to its value for the clean surface. It is important to note that at no time in our experiments did the yield from Al atoms *exceed* the value for the clean surface, which would occur, for example, if Al atoms were moving off of fcc lattice sites.[2–6]

To model the Ti film growth, the measured rate at which the number of visible Al atoms decreases with Ti coverage is compared with the decrease in the Al yield obtained from VEGAS computer simulations (solid circles in Figs. 2 and 3). First, we note that the yield obtained from the simulations agrees with the measured number of visible Al atoms for the clean surface. Results from the simulations for Ti overlayers are generally below the experimental results. However, the *rate* of attenuation for the number of visible Al atoms obtained from the simulations, 1.1 ML of Al per deposited Ti ML, agrees with the average attenuation rate obtained from the experiment *after the initial monolayer*. This attenuation of Al yield is strong evidence for pseudomorphic Ti epitaxial growth.

The change in the Al $2p$ photopeak areas as a function of Ti coverage, shown in Fig. 5, was modeled using an ideal layer-by-layer growth mode.[16] The attenuation of the intensity after the completion of h ML, plus an additional partial coverage x of the topmost layer, is described by $I_{\mathrm{Al}}=w^h(1-x+xw)$. Here, I_{Al} is the photopeak intensity, normalized to the intensity for the clean Al substrate; w is an attenuation factor expressed as $\exp[-d/(\lambda\cos\theta)]$, where d and λ are the interplanar distance in the overlayer and the attenuation length of electrons, respectively; θ is the photoelectron exit angle relative to the surface normal (30° in this case). The solid curve in Fig. 5 is a least-squares fit to the data in the region between 1 and 5.5 ML of Ti coverage. The inelastic mean free path was allowed to vary during the fitting procedure. We did not include the submonolayer data in this model fit because the lack of shadowing at low coverage in Figs. 2 and 3 and the lack of attenuation below 1 ML in Fig. 5 do not support an overlayer growth model. We also did not include the region above 5.5 ML in the fit because the HEIS (Fig. 2) and XPD (Fig. 6) results suggest that the structure of the film is changing in this coverage regime. Extending the layer-by-layer model fit to higher Ti coverages in Fig. 5 could be accomplished by using a larger value for λ, but this seems inappropriate since the morphology of the film may be changing, e.g., through the formation of islands. The resulting value of λ from the fitting in Fig. 5 was 13 Å. We do not consider this observation as strong evidence of a flat Ti film because of the ambiguity in the value of λ. Consequently, the HEIS and XPD results remain the crucial confirmation for Ti epitaxy on the Al surfaces for Ti coverages up to 5.5 ML.

The results obtained from off-normal rocking curves (Fig. 4) can be used to further characterize the epitaxial structure of the Ti film. In particular, these curves are used to measure the interplanar distance in the Ti overlayer. In the discussion above, our conclusions were based on the observed Ti-Al shadowing in the normal incidence channeling geometry. Although the shadowing depends on the Ti-Ti interatomic distance in the overlayer, this dependence is relatively weak, and thus cannot be used to evaluate the lattice constant $a_\perp$ in the Ti film. However, in the off-normal alignment the angular position of the minimum of the rocking curve near [101] for an epitaxial Ti film with a lattice constant identical to that of Al would coincide with the minimum of the Al rocking curve at an angle of 45° from the surface normal. On the other hand, stretched or contracted overlayer lattice constants lead to shifts in the angular locations of the minimum scattering yield from the overlayer as compared to that of the substrate. As shown in Fig. 4, the minimum yield for the 5 ML Ti film (maximum shadowing) occurs at 44.33°, as compared to the location of the Al minimum yield at 45° due to channeling along the [101] direction. Using this difference and the Al lattice constant, we obtain a value of 2.073 Å for $a_\perp$, the average (001) interplanar distance in the Ti film, as compared to 2.025 Å for Al, a difference of 2.4%. It should be noted that this measurement is an average of the overlayer lattice constant. In reality, the lattice constant may vary in a strained overlayer, where it adapts to the substrate structure at the interface and gradually relaxes as a function of distance from the substrate surface.

Our choice of using the Al bulk dechanneling yield to plot the Al rocking curve instead of the Al SP area is significant. As we indicated earlier, the background subtraction method introduces some uncertainties in the measured SP areas. This problem becomes worse when the beam is off axis because of an increased background behind the surface peak. In ad-

dition, the Al atoms near the surface may be strained because of the Ti overlayer, and thus the surface structure may not be a good reference for comparison. On the other hand, the variations in the yield due to bulk dechanneling reflect the bulk symmetries and directions, and are thus more useful for a reference direction.

The results of the angular distribution curve of the Ti $2p$ photoemission peak area confirm our findings from HEIS. The curve in Fig. 6(b) exhibits a peak near the polar emission angle of 45° for the 3 ML Ti film. This peak coincides with the Al $2p$ photopeak enhancement along [101]. Such results illustrate the significance of the XPD measurements in complementing the ion scattering experiments. The Ti-Ti shadowing in a 3-ML-thick film is too small in the MeV ion energy range to accurately measure the overlayer atomic structure. Such a condition on the overlayer thickness is not a requirement in XPD. Also, a HEIS study of an adsorbate/substrate system may become complicated in the case where the adsorbate atom is lighter than that of the substrate due to the difficulty in extracting the net SP areas. However, the precision of the ion scattering measurement in the determination of the overlayer lattice constant is excellent when the elemental conditions are favorable because the angular width of the rocking curve is much less than that of the forward focusing peaks obtained in XPD with our instrumentation. For the 5 ML Ti film, an angular shift of about 1° is observed in the Ti XPD peak along [101] compared to the Al XPD peak. Thus, both techniques indicate a larger value of $a_\perp$ in the Ti overlayer.

To put the comparison between XPD and HEIS measurements of overlayer structure on a more quantitative basis, we performed single-scattering calculations of the XPD spectra. Details regarding the XPD technique and the calculations are described elsewhere.[15] As discussed in the references, the single scattering calculation does a good job of locating the XPD peak positions, although multiple scattering corrections are necessary to get the line shapes and relative peak amplitudes to agree with experiment. In Fig. 7 we show a series of calculations for a 5 ML Ti overlayer in the fcc structure. The interplanar spacing $a_\perp$ varies from 2.02 to 2.22 Å. To facilitate comparison with the calculations, a smoothly varying background has been removed from the experimental data. Also, the emission angles have been redefined so that normal emission is at 90° in this figure. The dominant peak near 45° in the calculated spectra shifts gradually to larger emission angles, i.e., closer to normal emission, as the interplanar spacing in the overlayer is increased. A quantitative comparison between calculated and measured spectra was carried out to determine the best value of $a_\perp$ based only on the position of the emission peak near 45°. Figure 8 shows the results of an R-factor analysis using the measured photoemission intensity for polar emission angles between 35° and 55°. In this case the R-factor is the sum of the absolute differences between calculated and measured values at each emission angle, divided by the sum of the measured values for the same emission angles.[15] Best agreement with the data (solid circles in Fig. 7), occurs for $a_\perp = 2.12$ Å, a lattice expansion of 4.7% relative to that of clean Al. This expansion should be compared with the value of $a_\perp = 2.073$ Å (2.4% expansion) obtained with ion scattering.

So far we have considered the coverage regime in which

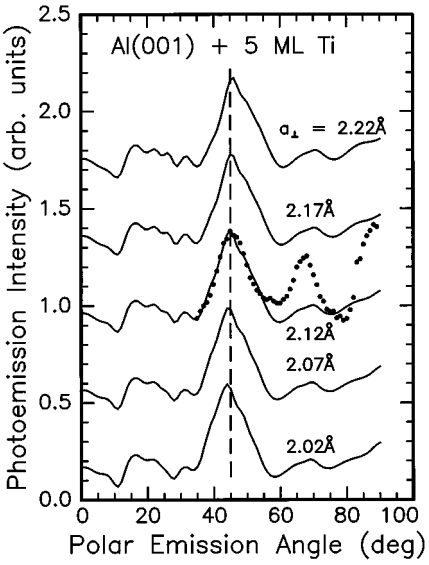

FIG. 7. Calculated (solid lines) and measured (solid circles) polar angle scans of Ti $2p$ photopeak intensity for a 5 ML Ti film on the Al(001) surface. Calculations for several interplanar distances are shown.

the Ti film grows epitaxially on the Al(001) substrate. From the HEIS results we obtain a value of about 5.5 ML for the critical film thickness, after which the structure undergoes a transformation to reduce the accumulated strain. This value is only slightly larger than that obtained for the growth of Ti on Al(110), where we obtained 5 ML for the measured critical thickness. The measured critical thickness on Al(001) is consistent with a lattice constant mismatch of 4%, where we have used the expression developed by Jesser and Kuhlmann-Wilsdorf.[17] This mismatch corresponds to an interatomic distance of 2.97 Å, as compared to 2.86 Å, the nearest-neighbor distance in Al. The value of 2.97 Å is close to the nearest-neighbor distance in the hexagonal close-packed structure of Ti (2.95 Å). Although bulk fcc Ti does not exist in nature, it is reasonable to start with the assumption that it would have the same interatomic distance as in the hcp structure.

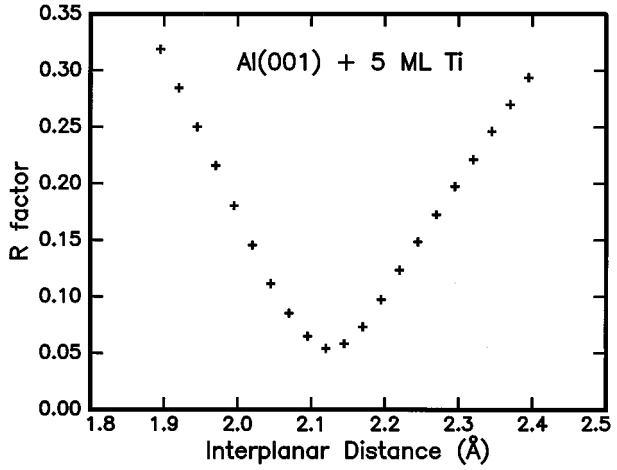

FIG. 8. R-factor analysis for the interplanar distance in a 5 ML Ti film on Al(001), using the position of the dominant peak near 45° in the XPD results shown in Figs. 6 and 7.

After the completion of our work we became aware of LEED experiments for Ti films deposited on Al(001).[7] These authors conclude that Ti films thicker than 10 Å have a body-centered tetragonal structure which matches the bulk Al(001) in-plane spacing of 2.864 Å, and has a vertical interplanar spacing of 2.14 Å. They further show using a strain analysis that the structure must be a modification of an equilibrium fcc structure rather that a distorted bcc structure. Our values for the interplanar distance (2.073 Å from HEIS and 2.12 Å from XPD) are in good agreement with their value. Formation of fcc Ti has also been reported for Ni/Ti multilayers.[18]

For Ti coverages exceeding the critical thickness, the atomic structure of the films is more difficult to determine. The authors of Ref. 7 conclude that the strained fcc structure continues to grow to thicknesses exceeding 25 Å, although they allow for errors in coverage determination of as much as $\pm 50\%$. Our observations consist of continued attenuation of the substrate XPS signal, decreased Al shadowing in HEIS, and broadening of the Ti $2p$ XPD peak at 45°. These observations are consistent with a relaxation of the Ti film as the critical thickness is exceeded, and the onset of some disorder causing a loss of the XPD peak. At this time we cannot reconcile the loss of the XPD peak for our thicker films with the well-developed 1×1 LEED pattern reported in Ref. 7. However, we are in good agreement for the structure of the thinner Ti films.

Finally, we return briefly to the structure of the Ti film for *submonolayer coverages*. Titanium films grown on the Al(110) surface appear to shadow Al atoms from the onset of deposition, i.e., they occupy sites directly above the Al surface atoms. On Al(001) surfaces, however, both the XPS attenuation curve (Fig. 5) and the HEIS shadowing (Figs. 2 and 3) indicate that Ti atoms may be intermixing with the surface Al atoms to form a surface alloy. Evidence for different behavior on the two surfaces is also reported in LEED studies where a weak $c(2\times2)$ pattern is seen for Ti/Al(001) while no such pattern is seen for Ti/Al(110).[7] Considerations of the higher surface energy for Ti would support the indiffusion of Ti on both Al surfaces, but does not distinguish adequately between them. Saleh and coworkers have reported low-energy ion scattering measurements which suggest that on the (001) surface the Al atoms do float on top of the Ti film and are only gradually incorporated into the Ti structure.[19] Similar experiments have not yet been made for the Al(110) surface. This gradual incorporation of Al atoms would explain the behavior seen in Figs. 2 and 3 where the measured HEIS yield gradually approaches the simulated curve, for example around 4 ML of Ti coverage. It may also help to explain any discrepancies between the XPD calculations and experiment shown in Fig. 7. Additional measurements are needed to determine the structure of the Ti films at submonolayer coverages on these Al surfaces.

In summary, we conclude that thin Ti films grow epitaxially on Al(001) surfaces in a fashion similar to that observed in the growth on Al(110) surfaces. The Ti atomic structure seems to perfectly match the Al fcc lattice in the directions parallel to the surface plane. A 2.4% distortion is observed for the fcc lattice in the direction perpendicular to the surface plane. A critical thickness of 5.5 ML is obtained for the Ti film, which is consistent with the mismatch between the Al crystal structure and an fcc Ti structure with 2.97 Å for the nearest-neighbor distance, similar to that of the bulk hcp Ti structure. Beyond the critical thickness, axial alignment with the substrate is only partially preserved, and off-normal alignment is lost according to our XPD measurements. The disorder in the film at coverages larger than the critical thickness may be associated with the formation of misfit dislocations or the relaxation to the hcp phase of Ti.

ACKNOWLEDGMENTS

The authors are pleased to acknowledge the technical support of Erik Andersen and Norm Williams, and valuable discussions with Lisa Peterson and Franco Jona. This work was supported by the National Science Foundation under Grant No. DMR-9409205, and by NASA EPSCoR Grant No. NCCW-0058. The work at Pacific Northwest Laboratories was supported under Contract No. DE-AC06-76RLO 1830.

*Present address: Charles Evans and Associates, 240 Santa Ana Court, Sunnyvale, CA 94086.

†Present address: Department of Mechanical Engineering, Tuskegee University, Tuskegee, AL 36088.

[1] Adli A. Saleh, V. Shutthanandan, and R. J. Smith, Phys. Rev. B **49**, 4908 (1994).

[2] V. Shutthanandan, Adli A. Saleh, N. R. Shivaparan, and R. J. Smith, Surf. Sci. **350**, 11 (1996).

[3] N. R. Shivaparan, V. Shutthanandan, V. Krasemann, and R. J. Smith, Surf. Sci. **373**, 221 (1997).

[4] V. Shutthanandan, Adli A. Saleh, and R. J. Smith, J. Vac. Sci. Technol. A **11**, 1780 (1993).

[5] V. Shutthanandan, Ph.D. thesis, Montana State University, 1994.

[6] N. R. Shivaparan, V. Krasemann, V. Shutthanandan, and R. J. Smith, Surf. Sci. **365**, 78 (1996).

[7] S. K. Kim, F. Jona, and P. M. Marcus, J. Phys.: Condens. Matter **8**, 25 (1996).

[8] L. C. Feldman, J. W. Mayer, and S. T. Picraux, *Material Analysis by Ion Channeling* (Academic, New York, 1982).

[9] J. F. van der Veen, Surf. Sci. Rep. **5**, 199 (1985).

[10] R. J. Smith, C. N. Whang, Xu Mingde, M. Worthington, C. Hennessy, M. Kim, and N. Holland, Rev. Sci. Instrum. **58**, 2284 (1987).

[11] D. J. Friedman and C. S. Fadley, J. Electron Spectrosc. Relat. Phenom. **51**, 689 (1990).

[12] J. W. Frenken, R. M. Tromp, and J. F. van der Veen, Nucl. Instrum. Methods Phys. Res. B **17**, 334 (1986).

[13] D. S. Gemmell, Rev. Mod. Phys. **46**, 129 (1974).

[14] Cheng Huan-Sheng, Chui Zhi-Xiang, Xu Hong-Jie, Yao Xiao-Wei, and Yang Fu-Jai, Nucl. Instrum. Methods Phys. Res. B **45**, 424 (1990).

[15] S. A. Chambers, Surf. Sci. Rep. **16**, 261 (1992); Adv. Phys. **40**, 357 (1991).

[16] S. Ossicini, R. Memeo, and F. Ciccacci, J. Vac. Sci. Technol. A **3**, 387 (1985).

[17] W. A. Jesser and D. Kuhlmann-Wilsdorf, Phys. Status Solidi **19**, 95 (1967).

[18] A. F. Jankowski and M. A. Wall, J. Mater. Res. **9**, 31 (1994).

[19] Adli A. Saleh, N. R. Shivaparan, R. J. Smith, and L. D. Peterson, Bull. Am. Phys. Soc. **41**, 698 (1996).